

# **Combining soft-SAFT and COSMO-RS modeling tools to assess the CO<sub>2</sub>-SO<sub>2</sub> separation using phosphonium-based ionic liquids**

G. Alonso<sup>1</sup>, P. Gamallo<sup>1\*</sup>, R. Sayós,<sup>1</sup> and F. Llovell,<sup>2\*</sup>

<sup>1</sup>Departament de Ciència de Materials i Química Física & Institut de Química Teòrica i Computacional (IQTUB), Universitat de Barcelona, C. Martí i Franquès 1, 08028 Barcelona, Spain.

<sup>2</sup>Department of Chemical Engineering and Materials Science. IQS School of Engineering, Universitat Ramon Llull, Via Augusta 390, 08017, Barcelona, Spain

\*Corresponding authors: [gamallo@ub.edu](mailto:gamallo@ub.edu)  
[felix.llovell@iqs.edu](mailto:felix.llovell@iqs.edu)

## ABSTRACT

The development of efficient CO<sub>2</sub> separation techniques from post-combustion flue gases is a key area of research to green-house gas control. However, CO<sub>2</sub> capture is typically affected by the presence of other acid impurities, such as traces of SO<sub>2</sub>. In that sense, this work assesses CO<sub>2</sub> separation from a CO<sub>2</sub>/SO<sub>2</sub> mixture with a set of phosphonium-based ILs. Two different modeling tools, soft-SAFT and COSMO-RS, have been used cooperatively to study the CO<sub>2</sub> gas separation on ILs. From one side, the soft-SAFT equation of state, which has been employed for the first time in this family of ILs, has been used to effectively reproduce the absorption properties of these promising CO<sub>2</sub> absorbents in a wide range of pressures/temperatures. Additionally, COSMO-RS, employed to evaluate the charge distribution so as to develop representative models for soft-SAFT, has been capable of reproducing the low-pressure absorption region in a purely predictive way. In both cases, the enthalpy and entropy of dissolution and the selectivity of the mixtures are predicted. Also, several ternary diagrams have been built to analyze different acid gas compositions.

## 1. INTRODUCTION

Ionic liquids (ILs) are salts that remain liquid at a temperature below 100 °C. In general, ILs present good physicochemical properties for industrial applications such as: low vapor pressure, high stability (i.e., both chemical and physical), low corrosivity and non-flammability [1–3]. They are formed by a cation/anion pair and any member can be exchanged to modify the properties of the fluid. This high tunability makes ILs a very interesting set of compounds to develop many specific tasks. Among others, several studies were devoted in the recent years to find optimal cation/anion pairs for carbon dioxide (CO<sub>2</sub>) capture and separation for industrial applications [4–8], such as the flue gas of post-combustion processes. These processes usually generate by-products (e.g., sulfur dioxide, SO<sub>2</sub>) that can affect the selectivity of the CO<sub>2</sub> separation technologies [9]. Specifically, SO<sub>2</sub> tends to prevent regeneration of CO<sub>2</sub> capture solvents or solid microporous materials [9]. In this regard, the use of technologies than can be regenerated under the presence of SO<sub>2</sub> is mandatory.

To find the best cation/anion pair for this specific task, it is helpful to employ computational modeling to predict the physicochemical properties of IL/gas mixtures in a large range of pressures and temperatures, which can overcome the costs and difficulties of experimental measurements in these kinds of systems. Molecular-based equations of state (EoS) such as the Statistical Associating Fluid Theory (SAFT) [10,11], and more specifically the soft-SAFT version [12], has been able to successfully describe the phase equilibria of different ILs with several gas molecules. Specifically, in the last years, the soft-SAFT EoS was used to study gas absorption in a wide variety of anions (e.g., [BF<sub>4</sub>]<sup>-</sup>, [NTf<sub>2</sub>]<sup>-</sup>, [DCA]<sup>-</sup>, [SCN]<sup>-</sup>, [Ac]<sup>-</sup>, [MeSO<sub>4</sub>]<sup>-</sup>) combined with imidazolium [13–15] and pyridinium [16,17] cations. Finally, CO<sub>2</sub> and SO<sub>2</sub> absorption have also been recently studied with tetraalkylammonium and choline chloride salts in deep eutectic solvents with CO<sub>2</sub> and SO<sub>2</sub> [18–20].

SAFT-based EoS success in the previous examples is not only due to an accurate fitting of thermophysical properties of ILs, but also due to the coarse-grained molecular model used in the equation, which gives physical meaning to the adjustable parameters of the EoS and allows further predictions when no data are available. The equation accounts for the shape of the molecules, general dispersive interactions (i.e., which also depend on the molecular shape) and finally, directional hydrogen bonding and/or polar interactions. The physical meaning of these parameters even allows, in some situations, to transfer some of them from similar systems to reduce the number of parameters needed in the fitting of the EoS.

An alternative tool to SAFT-based EoSs is COSMO-RS [21,22]. The method obtains the activity coefficients of different species based on quantum chemical calculations combined with statistical thermodynamics, which means that it does not need any previous experimental data for fitting. This feature turns COSMO-RS into a purely predictive method ideal for liquid solvent screening, such as ILs. In fact, this technique was previously applied to many liquid-liquid equilibrium (LLE) and vapor-liquid equilibrium (VLE) systems with good predictive results [23–25], specially reproducing Henry's coefficients.

In this work, the capability of the phosphonium cation-based ILs for gas absorption and separation will be explored using both tools, soft-SAFT and COSMO-RS in a complementary manner. Currently, phosphonium-based ILs have been characterized using different equations of state by several authors, although they have never been modeled with soft-SAFT. Specifically, Mozaffari et al. [26,27] used a modified version of the Song-Mason EoS, while Ferreira et al. [28] employed three different equations for the same purpose (i.e., the Goharshadi–Morsali–Abbaspour and the Sanchez–Lacombe EoSs to reproduce experimental densities and the Vogel-Fulcher-Tammann correlation for the viscosities). Similarly, Tomé et al. [29] measured IL densities and then they fitted their data to a Sanchez-Lacombe model and to a modified cell model EoS. Hosseini et al., [30] used a perturbed hard-sphere EoS to predict volumetric properties of these ILs and their mixtures. And finally, COSMO-RS was employed by Banerjee et al. [31] to model  $[P_{6,6,6,14}][Br]$ ,  $[BF_4]$  and  $[NTf_2]$ . In addition to these contributions, other groups specifically modeled gas absorption in phosphonium based ILs. Carvalho et al. [32] used a Peng-Robinson EoS to evaluate the CO<sub>2</sub> absorption capacity of  $[P_{6,6,6,14}][Cl]$  and  $[NTf_2]$ . Similarly, Manic et al., [33] fitted a Peng-Robinson and the Cubic-Plus-Association EoS to model CO<sub>2</sub> solubility in the same ILs. Ramdin et al., [34] also used the Peng-Robinson EoS, but to evaluate the absorption capability of  $[P_{6,6,6,14}][Br]$ ,  $[DCA]$  and  $[PO_4]$ . In a different approach, Camper et al. [35] and Scovazzo et al. [36] measured the solubility of CO<sub>2</sub> in several ILs (i.e., including  $[P_{6,6,6,14}][Cl]$ ) and modeled their results with regular solution theory. Finally, the version of PC-SAFT was used by Canales et al. [37] to model gas solubility in toluene +  $[P_{2,2,2,8}][NTf_2]$ .

In particular, three different phosphonium-based ILs are modeled in this work (i.e., formed by the trihexyl(tetradecyl)phosphonium cation  $[P_{6,6,6,14}]^+$  and three different anions: the chlorine  $[Cl]^-$ , the bis(trifluorosulfonyl)imide  $[NTf_2]^-$  and the dicyanamide  $[DCA]^-$ ). Since these ILs are modeled for the first time using soft-SAFT EoS, COSMO-RS is used a complementary tool to obtain the best molecular parameters for the model. Also, the solubility of CO<sub>2</sub> and SO<sub>2</sub> will be analyzed with both methods, as well as the selectivity of CO<sub>2</sub> vs SO<sub>2</sub> in the three ILs. Additionally, a comparison of both methods in predicting the absorption isotherms, Henry's coefficients, enthalpies and entropies of absorption is performed. To that end, the work is organized as follows: (1) The molecular soft-SAFT models and further parametrizations are proposed based on COSMO-RS information and previous results found for other cations and are validated comparing with the available experimental data; (2) pure ILs thermophysical data is obtained with soft-SAFT EoS; (3) binary absorption isotherms of CO<sub>2</sub> and SO<sub>2</sub> are calculated with soft-SAFT and COSMO-RS along with the Henry's coefficients, selectivities from Henry's coefficients and enthalpies and entropies of absorption; and (4) ternary absorption diagrams (i.e., IL + CO<sub>2</sub> + SO<sub>2</sub>) are predicted with soft-SAFT EoS to determine gas selectivity including the effect of pressure and gas competition towards the different ILs.

## 2. THEORY

SAFT is a molecular-based equation of state rooted in statistical mechanics concepts, proposed by Chapman et al. [10,11], and based on the thermodynamic perturbation theory of Wertheim et al.[38–41] SAFT theory has become a very valuable tool because it is capable to describe the thermodynamic properties of complex fluids and its mixtures with highly directional interactions, such as hydrogen bonds. Due to its success, many versions from the original SAFT equation have been developed (e.g., soft-SAFT [12,42], PC-SAFT [43], SAFT-VR [44] or SAFT- $\gamma$  [45], among others). In this work, we have used the soft-SAFT EoS, which modifies the reference term of the original SAFT theory by a Lennard-Jones (LJ) dispersion term. The soft-SAFT equation has already been proved to successfully reproduce the thermophysical properties and gas capture capabilities of many ILs [14,16,17,46], even if coarse-grained models are used. In this approach, the EoS of a fluid is modeled by a chain of homonuclear segments with the possibility of having association sites. It is typically written in terms of the different microscopic contributions to the molar Helmholtz free energies according to Eq. (1),

$$\frac{A^{total}}{Nk_B T} = \frac{A^{ideal}}{Nk_B T} + \frac{A^{ref}}{Nk_B T} + \frac{A^{chain}}{Nk_B T} + \frac{A^{assoc}}{Nk_B T} + \frac{A^{polar}}{Nk_B T} \quad (1)$$

where  $A^{ideal}$  is the ideal gas Helmholtz function. The  $A^{ref}$  term includes the intermolecular attractive and repulsive contributions to the energy between each pair of segments using a spherical LJ potential. The term  $A^{chain}$  arises from the presence of covalent bonds between the different segments, forming chains.  $A^{assoc}$  gives the contribution to the free energy according to the statistical association of the different segments through some defined association sites. Finally,  $A^{polar}$  accounts for the polar interactions between different segments.

The LJ reference term for pure fluids includes two adjustable molecular parameters: the segment diameter ( $\sigma_{ii}$ ) and the dispersive energy ( $\varepsilon_{ii}/k_B$ ) between two segments (i.e., the subscript  $i$  refers to the fluid species). This contribution is calculated using the Johnson et al. equation fitted to LJ monomers simulation data [47]. If soft-SAFT is extended to mixtures, the van der Waals one-fluid theory is applied with the modified Lorentz-Berthelot mixing rules (Eq. (2) and Eq. (3)). Here,  $\eta_{ij}$  and  $\xi_{ij}$  (i.e.,  $i$  and  $j$  are different species) are the size and energy binary parameters, respectively. If both values are equal to one, the original Lorentz-Berthelot mixing rules are recovered, and the LJ reference term for mixtures is calculated without any additional fitting.

$$\sigma_{ij} = \eta_{ij} \left( \frac{\sigma_{ii} + \sigma_{jj}}{2} \right) \quad (2)$$

$$\varepsilon_{ij} = \xi_{ij} \sqrt{\varepsilon_{ii} \cdot \varepsilon_{jj}} \quad (3)$$

The chain and association terms come from Wertheim's theory and are formally equivalent in the different versions of SAFT. The former term (Eq. (4)) depends on the radial distribution function ( $g_{ij}^{LJ}$ ) of the fluid and the chain length adjustable parameter for each component in the mixture ( $m_i$ ). On the other hand, the latter term (Eq. (5)) depends on the total number of association sites of each component ( $M_i$ ), and the fraction of molecules not bonded to the site  $\alpha$  ( $X_\alpha$ ). Both expressions are indistinctly used for pure fluids and mixtures, where each component has a molar fraction of  $x_i$ .

$$\frac{A^{chain}}{Nk_B T} = \sum_i x_i (1 - m_i) \ln g_{ij}^{LJ} \quad (4)$$

$$\frac{A^{assoc}}{Nk_B T} = \sum_i x_i \sum_{\alpha} \left( \ln X_{\alpha,i} - \frac{X_{\alpha,i}}{2} \right) + \frac{M_i}{2} \quad (5)$$

To calculate  $X_{\alpha,i}$  in Eq. (5) one needs to adjust two parameters for each association interaction: the site-site bonding-volume of association  $K_{\alpha\beta,ii}^{HB}$  and the site-site association energy  $\varepsilon_{\alpha\beta,ii}^{HB}$ . These parameters are related to  $X_{\alpha,i}$  through a mass action balance (see Eq. (6) and Eq. (7)).

$$X_{\alpha,i} = \frac{1}{1 + \rho \sum_{j=1}^n x_j \sum_{\beta=1}^s X_{\beta,j} \Delta_{\alpha\beta,ij}} \quad (6)$$

$$\Delta_{\alpha\beta,ij} = K_{\alpha\beta,ij}^{HB} \left[ e^{(\varepsilon_{\alpha\beta,ij}^{HB}/k_B T)} - 1 \right] g_{ij}^{LJ} \quad (7)$$

$\alpha$  and  $\beta$  in Eqs. (6) and (7) refer to different association bonding sites, and  $\rho$  is the total density. The cross-association interaction for the site-bonding volume of association and site-site association energy can be obtained by means of the common Lorentz-Berthelot mixing rules, without the addition of binary parameters. However, it must be noted that, as the site-bonding volume of association is a volumetric magnitude ( $K_{\alpha\beta,ij}^{HB}(\text{\AA}^3)$ ), the arithmetic mixing rules are performed taking the cubic root of  $K_{\alpha\beta,ii}^{HB}$  and  $K_{\alpha\beta,jj}^{HB}$ , averaging them, and then cubing to revert back to volume.

$$K_{\alpha\beta,ij}^{HB} = \left( \frac{{}^3\sqrt{K_{\alpha\beta,ii}^{HB}} + {}^3\sqrt{K_{\alpha\beta,jj}^{HB}}}{2} \right)^3 \quad (8)$$

$$\varepsilon_{\alpha\beta,ij}^{HB} = \sqrt{\varepsilon_{\alpha\beta,ii}^{HB} \cdot \varepsilon_{\alpha\beta,jj}^{HB}} \quad (9)$$

The polar term accounts for the quadrupolar interactions of linear symmetrical molecules (e.g., CO<sub>2</sub>, N<sub>2</sub>, etc.), and it is calculated from the extension of the theory of Gubbins and Twu [48] to chain fluids from Jog et al. [49]. This term includes the quadrupole moment of the molecule ( $Q$ ) as a new parameter to the model. Additionally, Jog's theory assumes that the polar moments are localized upon certain segments of the chain and so it defines  $x_p$ , which is the fraction of segments in a chain that contains the quadrupole.

With the previous formalism, one can build a model within the soft-SAFT environment. If all the adjustable parameters are correctly fitted to reliable and extensive experimental VLE data, providing a set of values with physical sense according to the features of the molecule, thermophysical properties of mixture fluids can be predicted. To ensure the validity of the parameters it is interesting to test them against derivative properties, which provide a stringent test for any EoS [50,51]. In this work, the isothermal compressibility (i.e., variation of the fluid density,  $\rho$ , with pressure,  $P$ , according to Eq. (10)), and the thermal expansion coefficient (i.e., variation of the fluid density,  $\rho$ , with temperature,  $T$ , according to Eq. (11)) are predicted with soft-SAFT EoS.

$$k_t = \frac{1}{\rho} \left( \frac{\partial \rho}{\partial P} \right)_T = \left( \frac{\partial \ln \rho}{\partial P} \right)_T \quad (10)$$

$$\alpha_p = -\frac{1}{\rho} \left( \frac{\partial \rho}{\partial T} \right)_P = -\left( \frac{\partial \ln \rho}{\partial T} \right)_P \quad (11)$$

Finally, the surface tension of these systems is calculated applying the density gradient theory (DGT) [52–54] coupled to the soft-SAFT EoS. This theory obtains the Helmholtz energy of an inhomogeneous fluid from the calculation of the

Helmholtz energy density  $a_0(\rho)$  at local composition and a corrective term coming from a Taylor expansion around the local  $a_0$ . This corrective term depends on the local density of component  $i$  and the so-called influence parameter ( $c_{ij}$ ). Using this approach, assuming a planar interface perpendicular to the  $z$ -direction and neglecting the temperature dependence in  $c_{ij}$ , the surface tension can be written as a function of the equilibrium pressure and chemical potential of the system:

$$\gamma = \sum_i \sum_j \int_{-\infty}^{\infty} c_{ij} \frac{d\rho_i}{dz} \frac{d\rho_j}{dz} dz = 2 \int_{-\infty}^{\infty} \left[ a_0(\rho) - \sum_i \rho_i \mu_{0i} - p_0 \right] dz \quad (12)$$

As a complementary predicting tool, we have used the conductor-like screening model for realistic solvents implemented in ADF (ADF/COSMO-RS) [55,56] to obtain the absorption isotherms, which can be compared with the results obtained with soft-SAFT and the previous equations. COSMO-RS has recently become a very interesting tool because is capable of estimating chemical potentials almost solely from molecular geometries and Density Functional Theory (DFT) data [57–62]. This ability, in principle, permits COSMO-RS to be used in screening to find the best cation/anion combination for a specific task without needing previous experimental information. We refer the reader to the original articles of COSMO-RS [21,22] for a more complete explanation of its theoretical background. Otherwise, we will detail a few of the main ideas behind COSMO-RS and the main equations used to obtain equilibrium properties from DFT data.

In the COSMO scheme, the first step is to perform DFT calculations to optimize the geometry of a molecule in a continuum solvent that resembles a perfect/ideal conductor. During the optimization, the conductor affects the electronic density of the molecule as well as the electronic density of the molecule affects the conductor. In this process, COSMO builds a cavity around the molecule and calculates the screening charge density ( $\sigma$ ) at the surface of the cavity. The value of  $-\sigma$  coincides with the molecular charge density, so positive  $\sigma$  implies negative charge densities and vice versa. Then, COSMO-RS treats the screening charge density at the surface of the cavity and splits it onto segments distributed along this surface. At this step, the distribution of segments with a screening charge of  $\sigma$  can be plotted. This property is known as the  $\sigma$ -profile and can be connected to the chemical potential of a segment, with surface charge density  $\sigma$ , through Eq. (13).

$$\mu_s(\sigma) = -k_B T \ln \int p_s(\sigma) e^{-\frac{E_{int}(\sigma, \sigma') - \mu_s(\sigma')}{k_B T}} d\sigma' \quad (13)$$

This equation depends on the sigma-profile and on an interaction energy that is parameterized with a general set of parameters already fitted by Klamt et al. [63] to reproduce free energies of hydration, partition coefficients and vapor pressures of several molecules. These parameters are: i)  $a_{eff}$ , the effective contact area between two segments, ii)  $\alpha'$ , the interaction parameter, iii)  $c_{HB}$ , the hydrogen bond strength, iv)  $\sigma_{HB}$ , the distance threshold to form hydrogen bonds and v)  $\tau_{vdW}$ , an element specific parameter to account for the van der Waals interactions, and are all compiled in the interaction energy between two different segments ( $E_{int}(\sigma, \sigma')$ ). As previously stated, these are general parameters and do not need to be parameterized specifically for each system. The chemical potential of a solute ( $x$ ) in a solvent ( $S$ ) can be obtained integrating  $\mu_s(\sigma)$  along  $\sigma$  and considering the combinatorial term  $\mu_{c,s}^x$ , as it can be seen in Eq. (14).

$$\mu_s^x = \mu_{c,s}^x + \int P^x(\sigma) \mu_s(\sigma) d\sigma \quad (14)$$

From the chemical potential obtained through Eq. (14), any other phase equilibrium property of a solute-solvent mixture can be calculated (e.g., absorption isotherms). In addition to solubility predictions, the qualitative information of the  $\sigma$ -profiles was used to build realistic coarse-grained models for the ILs modeled with soft-SAFT EoS.

Finally, the Clausius-Clapeyron expression [64] is used to obtain the enthalpy (Eq. (15)) and entropy (Eq. (16)) of dissolution of the mixtures using the data obtained from soft-SAFT and COSMO-RS. Henry's coefficients are calculated from the slope of the absorption isotherm at very low pressures.

$$\Delta H_{dis} = R \left( \frac{\partial \ln P_i^{vap}}{\partial (1/T)} \right)_{x_i} \quad (15)$$

$$\Delta S_{dis} = -R \left( \frac{\partial \ln P_i^{vap}}{\partial \ln T} \right)_{x_i} \quad (16)$$

### 3. MOLECULAR MODELS

The accurate description of thermophysical properties with soft-SAFT EoS depends on the correct selection of a reliable coarse-grained model. In this work, we have modeled three compounds of the trihexyl(tetradecyl)phosphonium family:  $[P_{6,6,6,14}][Cl]$ ,  $[P_{6,6,6,14}][NTf_2]$  and  $[P_{6,6,6,14}][DCA]$ . All these compounds have a large cation with a long aliphatic chain ( $C_{14}$ ) and three shorter aliphatic chains ( $C_6$ ), all connected to a central phosphonium cation interacting with a small anion. For simplicity, we have represented all tetraalkylphosphonium ILs with a single non-ramified bead chain with the necessary association sites to reproduce the appropriate polar interactions. This approximation was successfully used in a previous work with tetraalkylammonium ILs [18].

A dual associative site, representing the cation/anion pair, has been considered in the three ILs, in consistency with previous soft-SAFT models [65]. This site can interact either with positively charged or negatively charged associative sites due to its dual nature. Additional sites were added according to the information obtained from the COSMO-RS  $\sigma$ -profiles, based on the charge distribution along the molecule. These profiles allow locating the molecular regions with high electrostatic potential. Then, these regions can be assumed to work as associative sites in the soft-SAFT modeling. Fig. 1a shows the COSMO-RS optimized structures of the  $[P_{6,6,6,14}]^+$  cation and the three anions, and Fig. 1b contains the abovementioned  $\sigma$ -profiles. From the whole figure it is worth noting that the cation has a spherically localized charge around the  $P$  atom, similarly to  $[Cl]^-$ . The dual site for  $[P_{6,6,6,14}][Cl]$  has been modeled as the P-Cl associative interaction. The  $\sigma$ -profiles do not show any extra charged regions, so no additional sites have been added to these species.  $[NTf_2]^-$  and  $[DCA]^-$  are both symmetrical ions with a negative charge delocalized between the central N atom and two electronegative adjacent groups (i.e.,  $SO_2$  for  $[NTf_2]^-$  and  $CN$  for  $[DCA]^-$ ). Aside from the dual interaction represented by the cation-anion associative interaction, two additional sites are included to represent the groups where the negative charge is delocalized. To forbid associative interactions between the two negatively charged regions, these sites have been modeled to interact only with positive or dual sites but not with other negative charges.

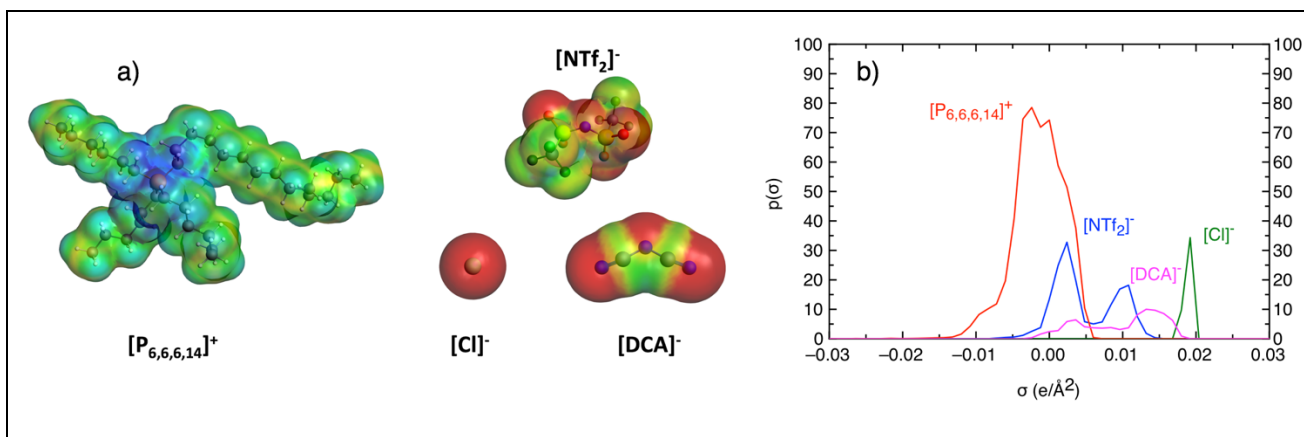


**Fig. 1.** (a) Electrostatic potential distribution for the [P<sub>6,6,6,14</sub>]<sup>+</sup> cation with a single positively charged region (blue). The [Cl]<sup>-</sup> anion shows a single negatively charged region (red). [NTf<sub>2</sub>]<sup>-</sup> and [DCA]<sup>-</sup> show very similar electrostatic pattern, with a weak negative region in the central atom and two negatively charged groups symmetrically distributed around the central N. (b)  $\sigma$ -profiles of all species modeled in this work.

To reduce the number of adjustable parameters we have performed DFT calculations to determine a reasonable value for the strength ( $\epsilon_{\alpha\beta,ij}^{HB}/k_B$ ) and volume ( $K_{\alpha\beta,ij}^{HB}$ ) of the associative interactions. To that end, we have calculated the relative cation-anion interaction energies and equilibrium distances for the three [P<sub>6,6,6,14</sub>][X] ILs, as well as those of other compounds previously modeled and validated with soft-SAFT EoS [14,19,46]. Then, the different values of  $\epsilon_{\alpha\beta,ij}^{HB}/k_B$  and  $K_{\alpha\beta,ij}^{HB}$  of these compounds have been scaled to obtain the [P<sub>6,6,6,14</sub>][X] parameters. The scaling was done according to the calculated relative difference of cation-anion DFT interaction energies and equilibrium distances. Both, the dual-site and the negatively charged sites were assumed to have the same parameters because the electronic density is delocalized along all the sites. For more details about the DFT calculations, the reader is referred to Section S1 of the Supplementary Information. The rest of the soft-SAFT adjustable parameters (i.e.,  $m$ ,  $\sigma$ ,  $\epsilon/k_B$ ) were fitted to experimental densities at different P and T conditions. To ensure that the proposed models for the different ILs and the fitted soft-SAFT parameters are able to capture the physics behind all the different interactions, we have compared liquid phase densities, isobaric compressibilities ( $\kappa_T$ ), thermal expansion coefficients ( $\alpha_P$ ) and vapor-liquid surface tensions ( $\gamma$ ), with their experimental counterparts at different pressures and temperatures based on the available experimental data in the bibliography.

The molecular model and parameters for CO<sub>2</sub> and SO<sub>2</sub> were obtained from previous works [66,67]. CO<sub>2</sub> does not bear any associative site, but its quadrupole is considered with an  $x_p = 1/3$ . On the other hand, the dipole of SO<sub>2</sub> is modeled with two associative sites representing the partially positively and partially negatively charged regions of the molecule. Moreover, any associative site of SO<sub>2</sub> can interact with the dual sites of all ILs, whereas the negative site of ILs can only interact with the positive site of SO<sub>2</sub>.

## 4. RESULTS AND DISCUSSION

**4.1 Soft-SAFT parameter fitting and pure IL thermophysical data:** Providing that ILs have a very low vapor pressure, the adjustable parameters of soft-SAFT EoS were fitted to single-phase liquid density data in a wide range of temperatures and pressures (i.e., T = 303 K – 333 K, and P = 0.2 MPa – 65 MPa). This is the common approach followed in previous

contributions when dealing with ILs [13–20,46,67–69]. Measured densities ( $\rho$ ) for the fitting of the ILs with  $[\text{Cl}]^-$  and  $[\text{NTf}_2]^-$  were obtained from the work of Esperança et al.[70] and the data for the IL with  $[\text{DCA}]^-$  were taken from Tomé et al.[29] The fitted parameters for all the species used in this work are compiled in Table 1. A comparison of the chain length ( $m$ ) for all studied members of the family reveals that the order of values agrees with the order of molecular volumes  $[\text{NTf}_2]^- > [\text{DCA}]^- > [\text{Cl}]^-$ . On the other hand, the anion had no significant effect to the segment diameter ( $\sigma$ ), so they were fixed at a constant value of 4.323 Å. Finally, the dispersive energies are very similar among the three ILs ranged as  $[\text{Cl}]^- > [\text{DCA}]^- > [\text{NTf}_2]^-$ . These results show that the cation is dominant in determining the segment diameter and dispersive energy soft-SAFT parameters due to its structure and presence of long aliphatic chains, whereas the anions have more impact on the chain length and association schemes. On the other hand, if the non-associative values fitted here (i.e.,  $m$ ,  $\sigma$  and  $\varepsilon/k_B$ ) are compared with other parameters obtained in previous works for other ILs [14,16–18,46], results that  $m$  is significantly larger,  $\sigma$  is slightly larger and  $\varepsilon/k_B$  is slightly lower.  $m$  is larger because of the significant difference in the molecular weight (i.e., from 519 g/mol for  $[\text{Cl}]^-$  to 764 g/mol for  $[\text{NTf}_2]^-$ ) and the chain length (i.e., a ramified  $\text{C}_{14}$  chain) of this family of compounds in contrast to other ILs (e.g., 200-400 g/mol for imidazolium-based and pyridinium-based ILs). The effect of  $[\text{P}_{6,6,6,14}]^+$  ramification was captured with an increase of the chain-segment molecular diameter ( $\sigma$ ). This feature was also seen in the previously mentioned tetraalkylammonium salts work [19]. Finally,  $\varepsilon/k_B$  is lower because, as mentioned, the cation has very long aliphatic chains that can only interact weakly with other species.

With respect the associative schemes, two types of sites have been considered: the dual site, which can interact with any site, and the negative sites, which are located in some anions. The associative pattern allows only dual-dual, dual-negative, dual-positive and negative-positive associative interactions, and their parameters can be found in Table 1.

**Table 1**

Soft-SAFT molecular parameters for ILs and gases used in this work. ILs parameters were obtained from fitting to experimental single-phase density data, while gas molecules were taken from previous contributions [66,67].

	$m$	$\sigma_{ii}$ (Å)	$\varepsilon_{ii}/k_B$ (K)	$\varepsilon_{\alpha\beta,ij}^{HB}/k_B$ (K)	$K_{\alpha\beta,ij}^{HB}$ (Å <sup>3</sup> )	$Q_{exp}$ (C/m <sup>2</sup> )	N of sites <sup>(1)</sup>	$c_{ij}$
$[\text{P}_{6,6,6,14}][\text{Cl}]$	11.231	4.323	386.25	3500	2000	-	1+0	8.998E-18
$[\text{P}_{6,6,6,14}][\text{NTf}_2]$	13.773	4.323	369.39	3300	2700	-	1+2	1.275E-17
$[\text{P}_{6,6,6,14}][\text{DCA}]$	11.836	4.323	379.86	3600	3000	-	1+2	1.000E-17
$\text{CO}_2$	1.571	3.184	160.2	-	-	4.4e-40 <sup>(2)</sup>	-	-
$\text{SO}_2$	2.444	2.861	228.3	1130	601	-	2	-

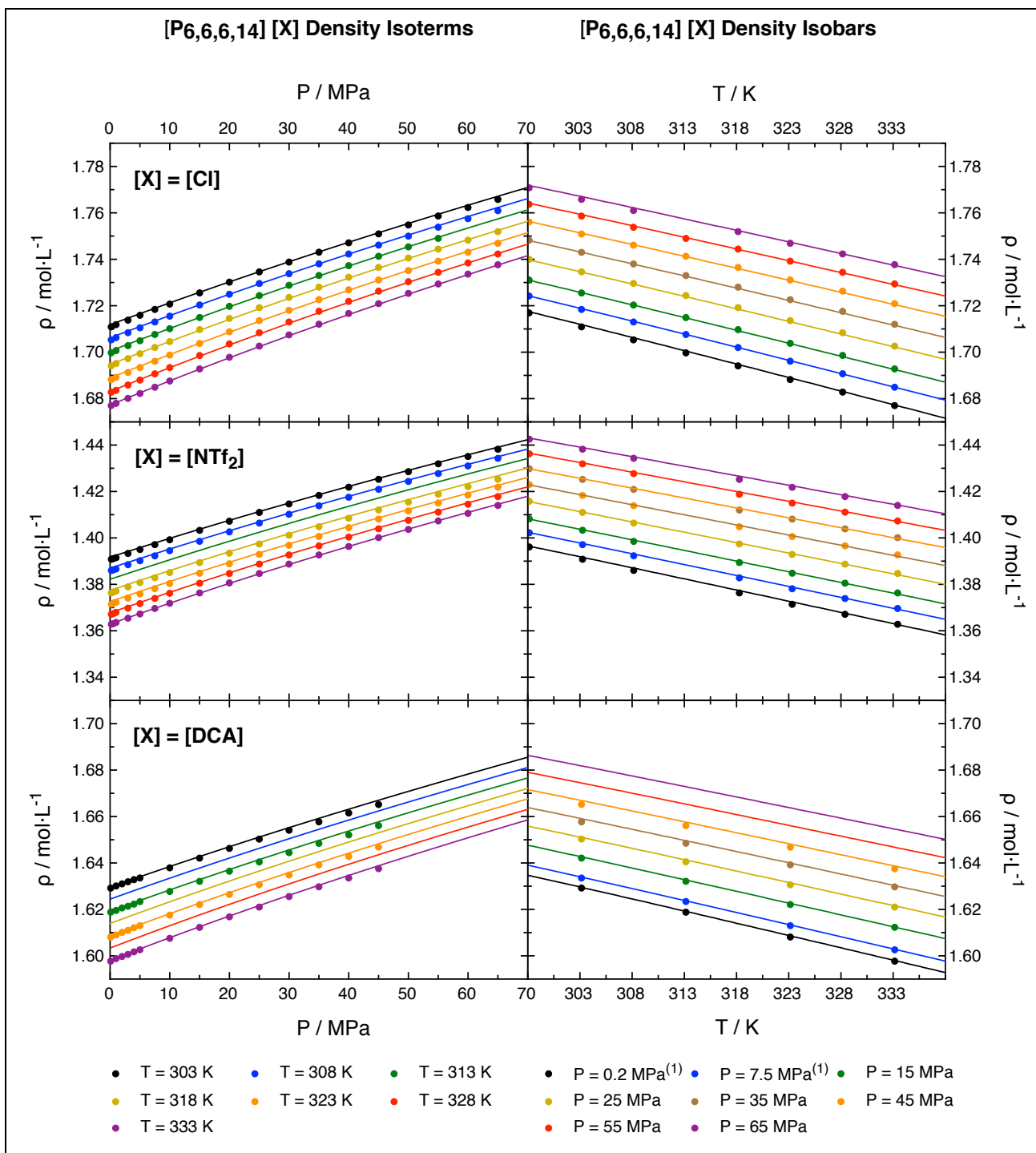
<sup>1</sup> the number of sites for ILs is separated into dual sites + negative sites. For example  $[\text{NTf}_2]^-$  is modeled with three sites, one of them is dual and the other two are negative (1+2). On the other hand,  $[\text{Cl}]^-$  is modeled only with a dual site, without negative sites (1+0).

<sup>2</sup>  $x_{p,\text{CO}_2} = 1/3$

After fitting the parameters for all the compounds, their validity against four pure IL properties have been tested: i) density, ii) isothermal compressibility, iii) thermal expansion coefficient and iv) surface tension. The results for these comparisons are plotted in Fig. 2, Fig. 3 and Fig. 4, respectively. The density at different pressures and temperatures for the three ILs is

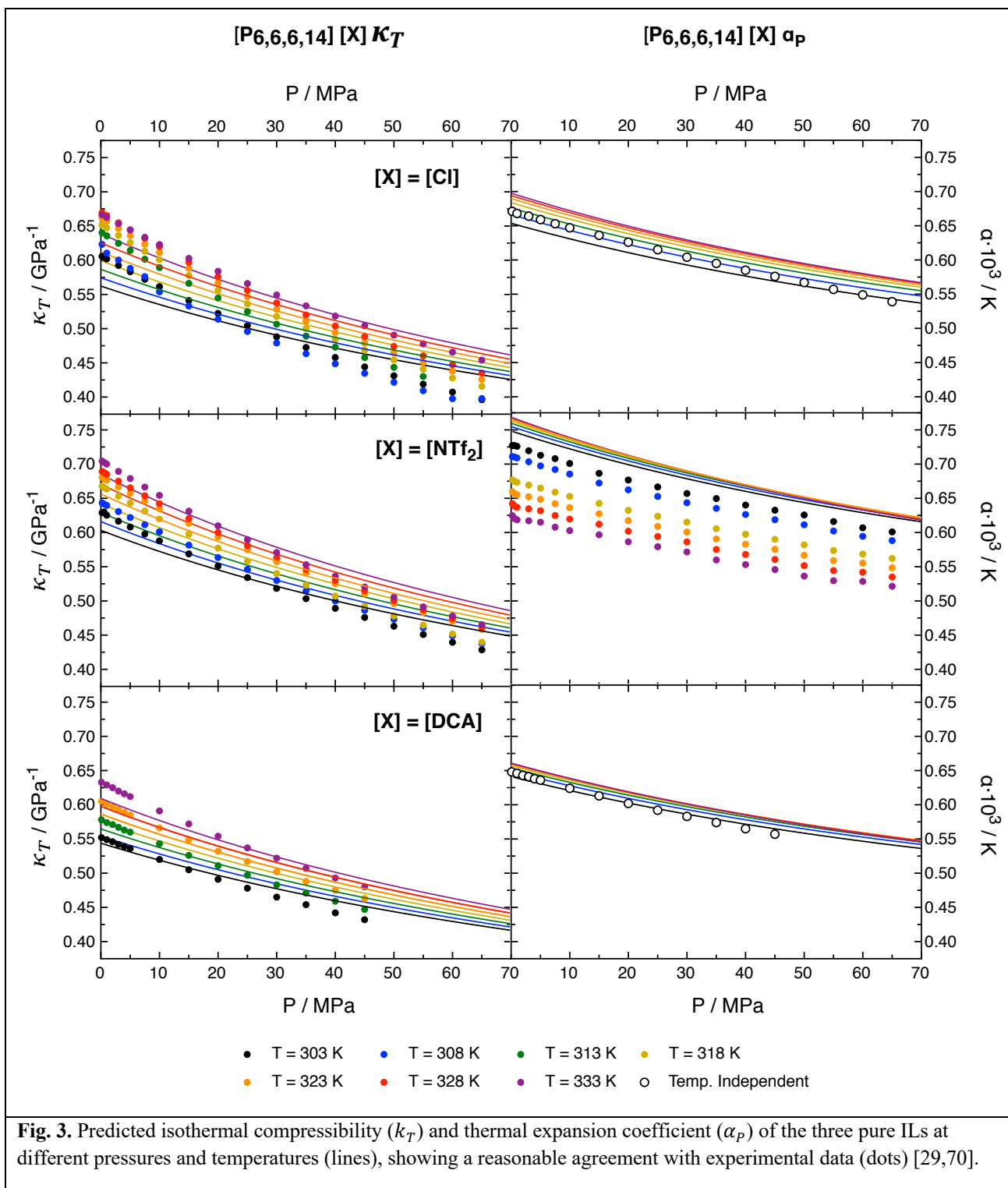
accurately reproduced with soft-SAFT EoS. The average absolute deviation (AAD%) in all the reproduced densities was less than 0.05%. For some few cases, as no data were available at the shown range of pressures and temperatures, the values were predicted with soft-SAFT.

Isothermal compressibilities ( $k_T$ ) at temperatures between 303 K and 333 K show a reasonably good agreement with the experimental information for all the ILs studied in this work [29,70]. Specifically, soft-SAFT EoS predicts very similar isothermal compressibilities for the three ILs, being  $[P_{6,6,6,14}][NTf_2]$  the one with higher values of  $k_T$  followed by  $[Cl]^-$  and  $[DCA]^-$ , respectively. This result is in qualitative agreement with the experimental data reported [29,70], which follows the same trend for this family of ILs. On the other hand, soft-SAFT EoS predicts low temperature dependencies on the  $\alpha_p$  values for all the studied ILs.  $[P_{6,6,6,14}][NTf_2]$  is the species with the highest  $\alpha_p$  values according to soft-SAFT followed by the other two ILs (i.e.,  $[Cl]^- > [DCA]^-$ ). The values of the latter ILs show very good agreement with the temperature independent experimental values reported by Esperança et al.,[70] and Tomé et al.,[29] for  $[P_{6,6,6,14}][Cl]$  and  $[DCA]$ , respectively. On the other hand,  $\alpha_p$  values obtained for  $[P_{6,6,6,14}][NTf_2]$  exhibit a higher deviation with respect the experimental data of Esperança et al.[70] In this case, soft-SAFT EoS is only capturing a  $\alpha_p$  value larger than the other ILs, which is in agreement with the experimental information, but not its temperature dependent behavior. Additionally, higher values of  $\alpha_p$  are predicted at higher temperatures, whereas the experimental trend is the opposite. This behavior was also seen in previous modeling works with soft-SAFT EoS with associative fluids, where the temperature dependence in the  $\alpha_p$  shows an inversion point [71]. This inversion is very sensitive to the chosen molecular parameters and normally, it can only be qualitatively represented, as shown by Crespo et al.[71]. Finally, the influence parameter ( $c_{ij}$ ) of the DGT (Eq. (12)) was fitted and the results were compared to the experimental values of Kilaru et al.[72] The experimental surface tension values lie close to each other around 33-35 mN/m and decrease with temperature. The soft-SAFT + DGT provides good agreement in all cases. Even though the slope of the calculated surface tension is slightly lower than the trend observed in the experimental work, the adequate pattern is captured. In summary, the overall description is good for all properties, validating the coarse-grained model proposed for all ILs.



**Fig. 2.** soft-SAFT predicted density (lines) at different pressures and temperatures compared to experimental data (dots) [29,70].

<sup>1</sup> Regarding the isobars for  $[\text{Cl}]^-$  and  $[\text{NTf}_2]^-$ , the black and blue dots correspond to reported experimental values at 0.2 and 7.5 MPa respectively. However, in the case of  $[\text{DCA}]^-$  the exact points were not reported, so the black and blue isobars correspond to the closest reported values (i.e., 0.1 and 5 MPa, respectively).



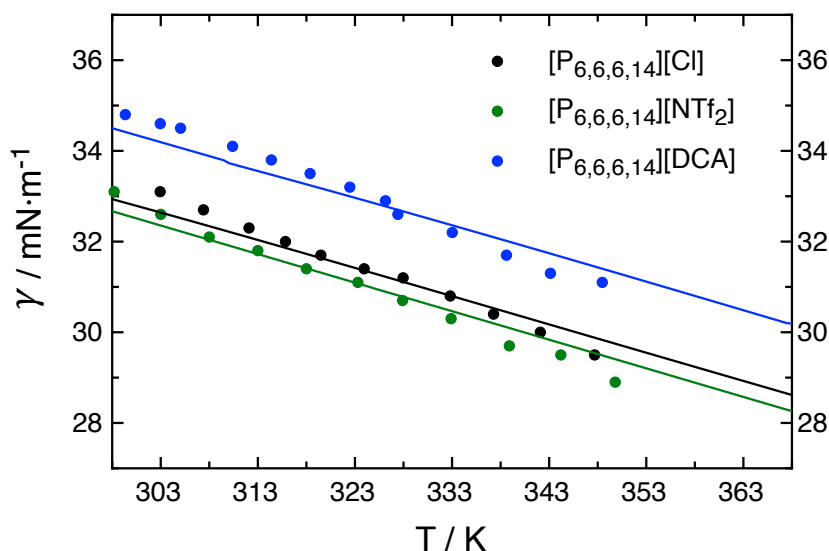


**Fig. 4.** Soft-SAFT predicted (lines) surface tension of [Cl]<sup>-</sup>, [NTf<sub>2</sub>]<sup>-</sup> and [DCA]<sup>-</sup> at different temperatures in comparison with experimental data (dots) from Kilaru et al [72].

**4.2 Gas absorption in ILs with soft-SAFT EoS and COSMO-RS:** After the definition of the pure ILs molecular models and the characterization of some of their basic thermodynamic properties, this section is focused on the analysis of CO<sub>2</sub> and SO<sub>2</sub> absorption in the three studied ILs for application in carbon capture and gas separation. To improve the representability of the results and obtain more insight on these systems, two different methods were employed to determine the absorption isotherms: (i) soft-SAFT EoS, whose energy binary parameter,  $\xi$ , was fitted to reproduce properties of ILs from moderate to high pressures (i.e., 0.2 MPa – 65 MPa), and (ii) COSMO-RS, which uses a general purpose set of parameters, the geometry and electron density of the molecules (i.e., that can be calculated from a DFT calculation) as input for phase equilibria calculations. The former requires experimental data, not only to fit and validate pure IL parameters, but also to adjust the gas/IL energy binary interaction parameter in equation (3), whereas the latter uses as input the screening charge density obtained via a DFT calculation and a set of pre-adjusted parameters.

Experimental data of CO<sub>2</sub> absorbed onto [P<sub>6,6,6,14</sub>][Cl] and [NTf<sub>2</sub>] from Ramdin et. al. [34] and [P<sub>6,6,6,14</sub>][DCA] from Carvalho et al. [32] were available to fit the soft-SAFT gas/IL binary parameters. Typically, an intermediate isotherm is used to fit the binary parameter and the value is transferred to other temperatures. In this work, the gas/IL binary interaction parameter ( $\xi_{ij}$ ) for CO<sub>2</sub> in [P<sub>6,6,6,14</sub>][Cl], [NTf<sub>2</sub>] and [DCA] is fitted to 0.940, 0.932 and 0.917, respectively, to reproduce the experimental information. These three values are comparable to other similar ILs already modeled by the soft-SAFT EoS (Ojeda et al.,[18] who used a  $\xi_{ij} = 0.947$  value for tetrabutylammonium chloride, or Pereira et al.,[14] who fitted a value of  $\xi_{ij} = 0.972$  for [C<sub>4</sub>mim][NTf<sub>2</sub>]). In any case, values lower than unity mean that the Lorentz rule would slightly overestimate the gas/IL interactions and the solubility of CO<sub>2</sub>.

SO<sub>2</sub>/IL binary interaction parameters are also required to study SO<sub>2</sub> absorption in phosphonium based ILs, but the experimental information in this kind of systems is scarce due to the high affinity of SO<sub>2</sub> for associative solvents. For this reason, binary interaction parameters for the three ILs had to be derived from similar systems. Specifically, Ojeda et al.

[18] studied the absorption of CO<sub>2</sub> and SO<sub>2</sub> in tetraalkylammonium based ILs and proposed values of  $\xi_{ij} = 0.947$  and  $\xi_{ij} = 0.880$  for both gases, respectively. Then, the relationship between the two  $\xi_{ij}$  values is supposed to be similar in both tetraalkylammonium and tetralkylphosphonium ILs due to their similar geometry and electrostatic interactions, as seen in the previous DFT calculations. To that end, the SO<sub>2</sub>/IL binary parameters were approximated through rescaling the CO<sub>2</sub>/IL values in [P<sub>6,6,6,14</sub>][X] by the same scaling factor than in tetraalkylammonium ILs. Finally, binary interaction parameters between CO<sub>2</sub> and SO<sub>2</sub> to calculate solubility in ternary mixtures were obtained from Llovel et al. [17]. All these parameters are compiled in Table 2.

**Table 2**  
All gas/IL binary interaction parameters used in this work for Eq. (3).

$i$	$\xi_{i,CO_2}$	$\xi_{i,SO_2}$
[P <sub>6,6,6,14</sub> ][Cl]	0.940	0.873
[P <sub>6,6,6,14</sub> ][NTf <sub>2</sub> ]	0.932	0.866
[P <sub>6,6,6,14</sub> ][DCA]	0.917	0.852
CO <sub>2</sub>	-	1.065
SO <sub>2</sub>	1.065	-

The absorption isotherms from 303K to 363K for CO<sub>2</sub>, with both soft-SAFT and COSMO-RS are drawn in Fig. 5. According to soft-SAFT EoS, higher absorption uptakes are achieved with [P<sub>6,6,6,14</sub>][NTf<sub>2</sub>] at high pressures, followed by [Cl] and [DCA]. These results agree with the common trend observed among other ILs that propose [NTf<sub>2</sub>]<sup>-</sup> as a good anion for CO<sub>2</sub> absorption [73]. Additionally, soft-SAFT is capable of reproducing the overall shape of the available IL experimental absorption isotherms in a long range of pressures and temperatures with a single temperature independent binary interaction parameter. On the other hand, the isotherms predicted with COSMO-RS are all very similar among each other, regardless of the IL modeled. COSMO-RS seems to significantly overestimate the high-pressure CO<sub>2</sub> solubility and saturation points in all ILs according to experimental data, except for [P<sub>6,6,6,14</sub>][NTf<sub>2</sub>], whereas soft-SAFT gives a better representation of these magnitudes.

Fig. 5 also contains a magnification of the low-pressure/composition region of the isotherms at the top left of each plot. In this region, one can see that soft-SAFT EoS is not capturing the temperature dependence of the isotherm in all cases. In this work, soft-SAFT EoS was fitted to reproduce the properties of ILs in a relatively large range of pressures and temperatures, so it is capable to capture the overall shape of the isotherms at a cost of a poorer description of the low-pressure range. On the other hand, COSMO-RS is better capturing the shape and temperature dependence of this region only slightly underestimating the absorption isotherms. Obviously, soft-SAFT could be fitted to reproduce low-pressure absorption isotherms and outperform COSMO-RS, but the latter is able to reasonably capture the gas/IL solubility without needing to fit any system specific parameter (i.e., it only needs the sigma profile from a DFT calculation, and the general purpose fitted parameters already included in the model).

The absorption of SO<sub>2</sub> is also analyzed in Fig. 6. Both methods predict a high SO<sub>2</sub> solubility in all ILs. Soft-SAFT EoS predicts the highest SO<sub>2</sub> absorption with [P<sub>6,6,6,14</sub>][NTf<sub>2</sub>] and [Cl], whereas [P<sub>6,6,6,14</sub>][DCA] exhibits the lowest affinity

among these species. On the other hand, COSMO-RS results suggest that SO<sub>2</sub> interacts more strongly with [P<sub>6,6,6,14</sub>][Cl] and [DCA] than [P<sub>6,6,6,14</sub>][NTf<sub>2</sub>]. Again, COSMO-RS is predicting larger CO<sub>2</sub> and SO<sub>2</sub> high-pressure solubility and saturation points than soft-SAFT EoS. It is important to remark that, in both cases, the information given in Fig. 6 has been derived in an entirely predictive way due to the lack of experimental information.

**Table 3**

CO<sub>2</sub>/IL and SO<sub>2</sub>/IL Henry's coefficients along with the SO<sub>2</sub> selectivity towards CO<sub>2</sub> in the three studied ILs. Experimental values at 303 K have an experimental error of  $\pm 0.2$  MPa,  $\pm 0.8$  MPa and  $\pm 0.4$  MPa for [P<sub>6,6,6,14</sub>][Cl], [NTf<sub>2</sub>] and [DCA], respectively.

		$H_{CO_2}^{exp} / \text{MPa}$	$H_{CO_2} / \text{MPa}$			$H_{SO_2} / \text{MPa}$			$S_{SO_2/CO_2}$		
		303 K	303 K	333 K	363 K	303 K	333 K	363 K	303 K	333 K	363 K
soft-SAFT	[P <sub>6,6,6,14</sub> ][Cl]	3.04 [35]	2.71	3.81	5.36	0.10	0.25	0.49	27.1	15.2	10.9
	[P <sub>6,6,6,14</sub> ][NTf <sub>2</sub> ]	3.34 [74]	2.06	3.08	4.17	0.08	0.21	0.42	25.8	14.7	9.9
	[P <sub>6,6,6,14</sub> ][DCA]	2.97 [74]	2.73	4.11	5.53	0.12	0.30	0.59	22.8	13.7	9.4
COSMO-RS	[P <sub>6,6,6,14</sub> ][Cl]	3.04 [35]	2.54	4.05	6.44	0.10	0.20	0.35	25.4	20.3	18.4
	[P <sub>6,6,6,14</sub> ][NTf <sub>2</sub> ]	3.34 [74]	2.81	4.41	6.95	0.17	0.37	0.62	16.5	11.9	11.2
	[P <sub>6,6,6,14</sub> ][DCA]	2.97 [74]	2.78	4.42	6.30	0.12	0.27	0.48	23.2	16.4	13.1

From the slope of the absorption isotherms at  $x, P \rightarrow 0$  the Henry's coefficients of CO<sub>2</sub> and SO<sub>2</sub> have been calculated in the three ILs. As far as the absorption results have shown a higher capacity to absorb SO<sub>2</sub>, the selectivity of these ILs towards SO<sub>2</sub> with respect CO<sub>2</sub> can be calculated from the ratio of Henry's coefficients (i.e.,  $S_{SO_2/CO_2} = H_{CO_2}/H_{SO_2}$ ). This selectivity does not consider the effect of competition among species when calculated from the binary system, but it is a good approximation to determine gas/IL affinity. The results of Henry's coefficients and selectivity calculated with both, soft-SAFT EoS and COSMO-RS are listed in Table 3. In general, all ILs exhibit larger Henry's coefficients (i.e., lower affinity) for CO<sub>2</sub> than for SO<sub>2</sub>, which is related to a significantly bad IL selectivity for CO<sub>2</sub> related to SO<sub>2</sub> (i.e., and a high selectivity for SO<sub>2</sub> with respect CO<sub>2</sub>). This result shows that the three ILs studied would be easily saturated by SO<sub>2</sub>, capturing only a small portion of CO<sub>2</sub>. For this reason, if a mixed flue gas containing both gases is treated with any of the studied ILs, it is preferable to separate CO<sub>2</sub> by capturing SO<sub>2</sub> instead.

When comparing to the available experimental Henry's coefficients [35,74], both soft-SAFT and COSMO-RS are capable of giving similar and reasonable estimate values at 303 K for [P<sub>6,6,6,14</sub>][Cl] and [DCA]. However, soft-SAFT underestimates the Henry's coefficient of [P<sub>6,6,6,14</sub>][NTf<sub>2</sub>] by approximately 40%, whereas COSMO-RS only deviates a 15%. Additionally, the qualitative temperature dependence of Henry's coefficients is better reproduced by COSMO-RS because, as it was already seen in Fig. 5, the shape of the absorption isotherm at different temperatures in the low-pressure/composition region is generally well reproduced by this method. It is worth noting that the obtained Henry's coefficients are lower than other widely used imidazolium based ILs. Some examples at similar temperatures are [C<sub>4</sub>mim][PF<sub>6</sub>] with a Henry's coefficient of 5.71 MPa [75], [C<sub>4</sub>mim][BF<sub>4</sub>] with a value of 6.25 MPa [76] or [C<sub>2</sub>mim][DCA] with 9.60 MPa [77]. Some of the ILs with the lowest Henry's coefficients are the family of [C<sub>n</sub>mim][NTf<sub>2</sub>], with values very similar to the phosphonium based ILs here modeled (i.e., 4.01, 3.46 and 3.44 for n = 2, 4 and 6 respectively [78–80]). This means that all phosphonium based ILs have very good gas affinity, comparable to some of the most suitable imidazolium absorbents.

**Table 4**

Enthalpies and entropies of dissolution at low ( $x_{gas} = 10^{-3}$ , diluted) and high ( $x_{gas} = 0.75$ , concentrated) molar fractions of CO<sub>2</sub> and SO<sub>2</sub> obtained from the temperature dependence of the absorption isotherms for both methods.

			$\Delta H_{dis} / \text{kJ}\cdot\text{mol}^{-1}$		$\Delta S_{dis} / \text{J}\cdot(\text{mol}\cdot\text{K})^{-1}$	
			CO <sub>2</sub>	SO <sub>2</sub>	CO <sub>2</sub>	SO <sub>2</sub>
soft-SAFT	[P <sub>6,6,6,14</sub> ][Cl]	Diluted	-11.5	-24.4	-34.6	-73.6
		Concentrated	-13.1	-23.0	-39.6	-69.4
	[P <sub>6,6,6,14</sub> ][NTf <sub>2</sub> ]	Diluted	-10.6	-23.9	-31.6	-71.0
		Concentrated	-12.1	-23.0	-36.2	-68.4
	[P <sub>6,6,6,14</sub> ][DCA]	Diluted	-10.7	-24.1	-32.2	-72.6
		Concentrated	-12.5	-22.9	-37.6	-69.0
COSMO-RS	[P <sub>6,6,6,14</sub> ][Cl]	Diluted	-14.1	-18.6	-42.7	-56.0
		Concentrated	-12.7	-22.7	-38.3	-68.6
	[P <sub>6,6,6,14</sub> ][NTf <sub>2</sub> ]	Diluted	-13.9	-19.7	-42.0	-59.4
		Concentrated	-12.5	-22.1	-37.8	-66.6
	[P <sub>6,6,6,14</sub> ][DCA]	Diluted	-11.5	-20.5	-34.8	-61.7
		Concentrated	-12.6	-22.6	-37.9	-68.1

Enthalpies and entropies of dissolution at different gas compositions have also been calculated from the results obtained for both soft-SAFT EoS and COSMO-RS for all the studied ILs, using Eqs. (15) and (16), respectively. These properties provide information about the solute-solvent interaction strength and stability of the solution. As it can be seen in **Table 4**, the  $\Delta H_{dis}$  values for CO<sub>2</sub> are significantly lower than for SO<sub>2</sub>. This result shows again that all ILs have higher affinity for SO<sub>2</sub> than for CO<sub>2</sub>. Notice that the enthalpies of dissolution have only a slight dependency on the amount of gas dissolved in the IL, being the difference between the infinitely diluted values and the  $\Delta H_{dis}$  at gas molar fraction of  $x_i = 0.75$  less than 1 kcal/mol. Additionally, both soft-SAFT EoS and COSMO-RS have  $\Delta H_{dis}$  at high concentrations in very good agreement among each other, whereas the infinite dilution values exhibit larger deviations. Specifically, the infinitely diluted CO<sub>2</sub> has higher values of  $\Delta H_{dis}$  with COSMO-RS than soft-SAFT, whereas with SO<sub>2</sub> the opposite trend is observed. The calculation of entropies of dissolution shows very similar results with both methods at high gas concentration, with larger deviations in the low-pressure region. The results reveal that entropy is lost upon gas absorption and the difference between low and high gas concentrations is around 1 cal/mol·K in all cases.

In summary, the performance of both methods suggests that, for the studied systems, COSMO-RS is a suitable tool to obtain absorption properties at low-pressure regions, giving Henry's coefficients in good agreement with experimental information. However, the high-pressure region presents larger deviations from experiments. In these situations, it is more suitable to use the soft-SAFT EoS providing that a minimum amount of experimental data (i.e., at least one isotherm) is available to fit the required gas/IL binary interaction parameters. On the other hand, absorption enthalpies and entropies show very similar behavior with both methods at high gas concentration, whereas the values at the low-pressure regime have higher deviations. It is worth seeing that COSMO-RS is capable of reproducing the correct temperature dependence of the absorption isotherms without needing to fit any parameter, while soft-SAFT EoS fitted a single temperature-

independent parameter to reproduce a correct overall behavior at the cost of increasing the error at the specific low-pressure region. In any case, both approaches offer consistent, coherent and transferable results and can be used as complementary tools.

From a more applied perspective, and according to the obtained results, it is suggested that all ILs will become selectively saturated by SO<sub>2</sub> when mixed in a flue gas containing CO<sub>2</sub>. However, from the pure absorption isotherms of SO<sub>2</sub>, it can be concluded that the separation could be performed by capturing the contaminant at low pressures (e.g., 0.1-0.3 MPa) and low temperatures (e.g., 303 K), and then, it can be regenerated by heating the IL at atmospheric pressure and high temperatures (e.g., 363 K).

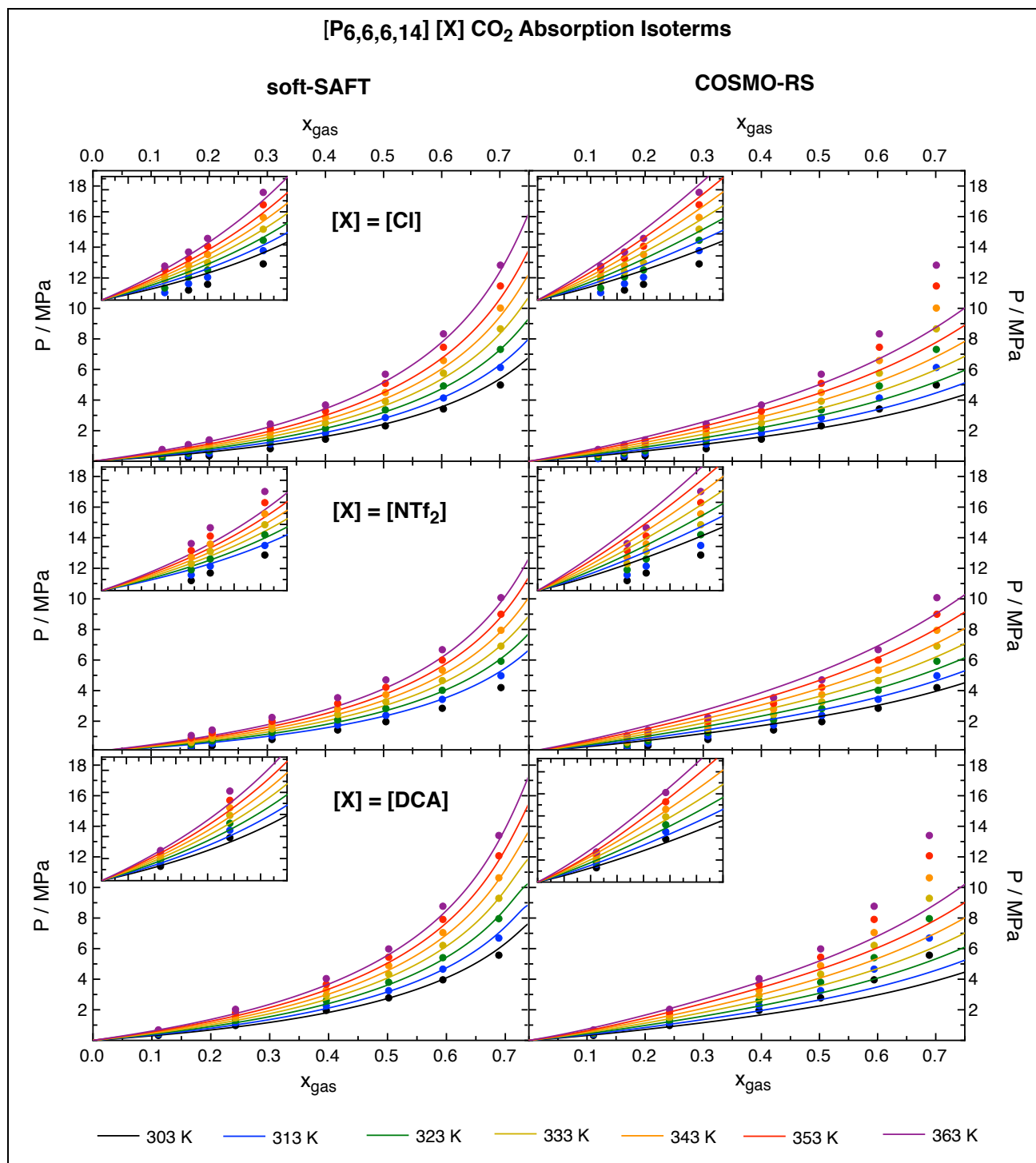
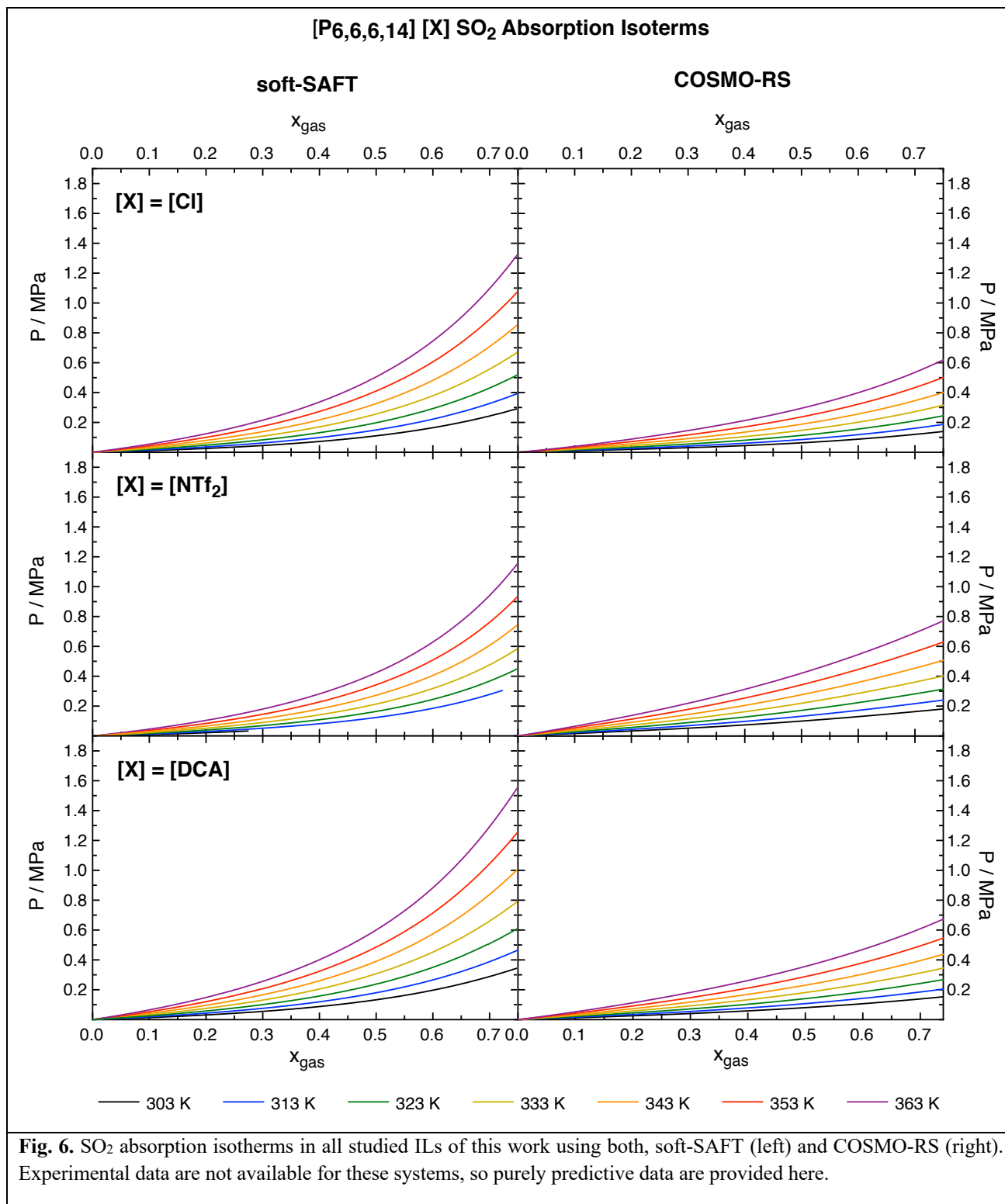


**Fig. 5.** CO<sub>2</sub> absorption isotherms in all studied ILs of this work using both, soft-SAFT (left) and COSMO-RS (right). Experimental data [29,70] is depicted with dots and a zoom of the low pressure/composition region is shown within each plot (i.e., from  $x_{gas} = 0$  to  $x_{gas} = 0.35$ ).



**4.3 CO<sub>2</sub>/SO<sub>2</sub> Competition Assessed from Ternary Mixtures:** The selectivity obtained from Henry's coefficients is an approximation based on infinite dilution behavior (i.e.,  $P \rightarrow 0$ ) and lack of absorption competition. To account for these factors, ternary mixtures containing both gases plus the IL have been modeled in this section. The temperature of 333 K and different pressures (i.e., from 0.1 MPa to 4.0 MPa) were selected as representative conditions of post-combustion flue gas mixtures. However, previously to the evaluation of the ternary gas mixtures, Llovell et al.,[17] computed with soft-SAFT EoS the CO<sub>2</sub>/SO<sub>2</sub> binary VLE. In that work, they were capable of successfully reproducing the experimental equilibrium data of the mixture at different temperatures, validating the model to describe the CO<sub>2</sub>/SO<sub>2</sub> VLE region at pressures higher than 1.0 MPa at 333K. In the ternary mixtures absorption isotherms shown in Fig. 7, the VLE lines for [P<sub>6,6,6,14</sub>][NTf<sub>2</sub>] are located at a composition with higher CO<sub>2</sub> content, which implies that the absorption capacity for CO<sub>2</sub> of this IL is higher compared to the other two ILs, as already seen when studying the binary systems. Overall, the equilibrium uptake of [P<sub>6,6,6,14</sub>][Cl] and [DCA] is similar and slightly lower than [P<sub>6,6,6,14</sub>][NTf<sub>2</sub>].

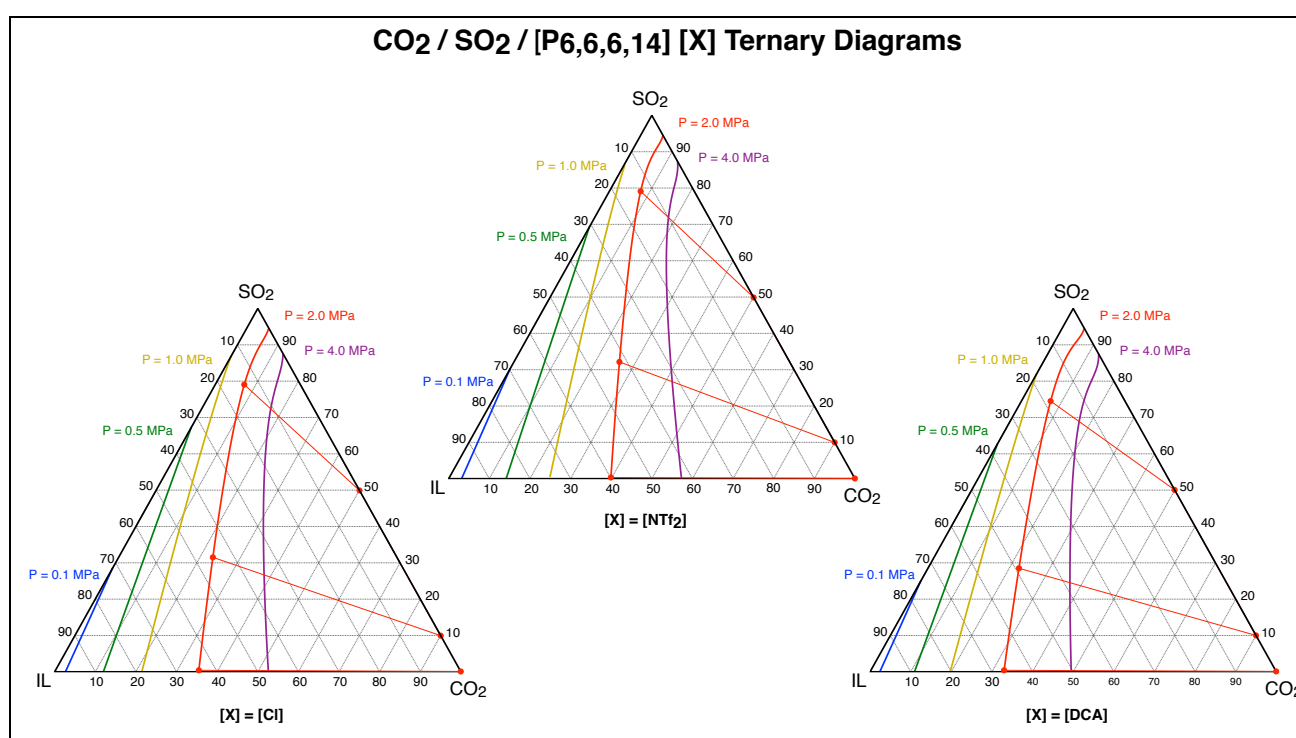


**Fig. 7.** CO<sub>2</sub>/SO<sub>2</sub>/IL ternary absorption isotherms for all studied ILs of this work at 333 K predicted by soft-SAFT EoS. Solid lines correspond to the isobaric frontiers between the liquid phase (left of the line) and the VLE region (right of the line) at pressures from 0.1 MPa up to 4 MPa. The frontier between the VLE and vapor phase almost corresponds to the binary CO<sub>2</sub>/SO<sub>2</sub> axis of the diagram due to the negligible the vapor pressure of all ILs. The connected dots correspond to the liquid and vapor phases at equilibrium with a flue gas composition (i.e., molar percentages) of 99.9% CO<sub>2</sub> and 0.1% SO<sub>2</sub>, 90% CO<sub>2</sub> and 10% SO<sub>2</sub> and 50% CO<sub>2</sub> and 50% SO<sub>2</sub>.

We have selected three different CO<sub>2</sub>/SO<sub>2</sub> gas mixtures with different composition: the first is CO<sub>2</sub> rich flue gas containing a 99.9% CO<sub>2</sub> and 0.1% SO<sub>2</sub>; the second is an intermediate mixture, which is still rich in CO<sub>2</sub> but with a higher SO<sub>2</sub> content (i.e., 90% CO<sub>2</sub> and 10% SO<sub>2</sub>); and finally, an equimolar mixture with 50% CO<sub>2</sub> and 50% SO<sub>2</sub>. Flue gas mixtures usually contain higher amounts of CO<sub>2</sub> than SO<sub>2</sub>, so the former composition is used to evaluate the capacity of the ILs to separate CO<sub>2</sub> and SO<sub>2</sub> in this situation. On the other hand, the latter composition compares the absorption capacity of ILs at equal

conditions, which would be similar to the Henry's coefficients previously calculated. The selectivity values calculated from these flue gas mixtures are obtained throughout Eq. (17) and are shown in Fig. 8.

$$S_{CO_2/SO_2} = \frac{x_{CO_2} y_{SO_2}}{x_{SO_2} y_{CO_2}} \quad (17)$$

where  $x$  is the molar fraction of each component at the absorbed phase and  $y$  is the molar fraction of each component at the gas phase. The selectivity values calculated from ternary mixtures at low pressures (i.e., 0.1 MPa) are comparable to the previously calculated values for binary mixtures. Although all ILs show higher selectivity towards  $SO_2$  than for  $CO_2$ , the increase of the pressure from 0.1 MPa to 4 MPa reduces the  $SO_2/CO_2$  selectivity approximately a 25-30%. This fact implies that an effective  $CO_2$  separation throughout  $SO_2$  capture would be carried out preferably at low pressures to increase the selectivity of these ILs towards  $SO_2$ . Even though  $[P_{6,6,6,14}][NTf_2]$  is the IL with higher absorption capacity,  $[P_{6,6,6,14}][Cl]$  shows the highest selectivity towards  $SO_2$  capture followed by  $[P_{6,6,6,14}][NTf_2]$  and  $[DCA]$ . Finally, the differences in selectivity in all gas compositions are not significant, but the equimolar mixture seems to be slightly less  $SO_2$  selective than the lower  $SO_2$  content gas mixtures.

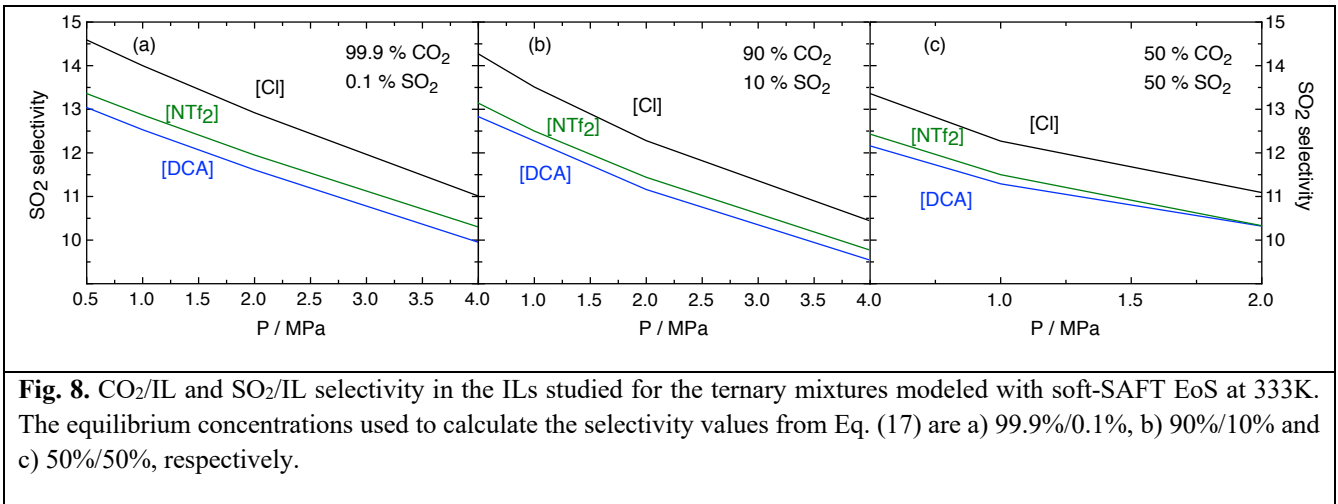


**Fig. 8.**  $CO_2/IL$  and  $SO_2/IL$  selectivity in the ILs studied for the ternary mixtures modeled with soft-SAFT EoS at 333K. The equilibrium concentrations used to calculate the selectivity values from Eq. (17) are a) 99.9%/0.1%, b) 90%/10% and c) 50%/50%, respectively.

## 5. CONCLUSIONS

In this work, we have used the soft-SAFT molecular-based equation of state to assess gas separation using phosphonium based ILs. The associative scheme of the coarse-grained models can be successfully constructed with the help of techniques based on DFT calculations (i.e., ADF/COSMO-RS), which allows identifying the molecular regions with a higher electrostatic potential and assign the associative sites for their accurate modeling. The resulting soft-SAFT models were validated through an adequate reproduction of many pure IL properties, such as density, isothermal compressibility, thermal expansion coefficient and surface tension.

COSMO-RS, which does not need to fit any system specific parameter to be used, and the soft-SAFT EoS were used to predict binary absorption isotherms. The results of the soft-SAFT EoS highlight the capacity of the approach to reproduce the equilibrium uptakes at several pressures and temperatures by fitting a single temperature independent binary interaction parameter, although this overall good description is at the cost of having some slight deviations at the low-pressure region in comparison with the experimental data. On the other hand, COSMO-RS was able to reasonably capture the shape of the absorption isotherms at low-pressure by an entirely predictive way, although this method significantly overestimated gas

absorption at higher pressures, obtaining a worse description of the whole isotherm. The results here compiled suggest that COSMO-RS is a good method to predict absorption properties at low pressures without needing to fit any parameters, whereas soft-SAFT can provide a better description at widespread conditions if a minimum amount of data are available to fit a binary interaction parameter.

The studied ILs have significantly high affinity for both CO<sub>2</sub> and SO<sub>2</sub> absorption, as it can be seen by the calculated Henry's coefficients. These values are comparable to some of the better ILs for CO<sub>2</sub> absorption such as [C<sub>x</sub>mim][NTf<sub>2</sub>]. Additionally, all ILs absorb SO<sub>2</sub> preferentially in a flue gas mixture containing both CO<sub>2</sub> and SO<sub>2</sub>. For this reason, it could be more efficient to separate the CO<sub>2</sub> by capturing SO<sub>2</sub> with these ILs. Even though [P<sub>6,6,6,14</sub>][NTf<sub>2</sub>] is the IL with the highest absorption capacity, the most efficient IL to perform this separation seems to be [P<sub>6,6,6,14</sub>][Cl]. The reason is that [P<sub>6,6,6,14</sub>][Cl] is the most SO<sub>2</sub> selective IL, according to the selectivity values derived either from the Henry's coefficients, (i.e., using both COSMO-RS and soft-SAFT) or from the ternary mixtures. This IL also has higher equilibrium uptakes than [P<sub>6,6,6,14</sub>][DCA], while it is overcome by [P<sub>6,6,6,14</sub>][NTf<sub>2</sub>]. The optimal gas separation conditions are an absorption stage of the flue gas with the contaminant at low pressures (e.g., 0.1-0.3 MPa) and low temperatures (e.g., 303 K), followed by a regeneration stage by heating the IL at atmospheric pressure and 363 K.

## ACKNOWLEDGEMENTS

GESPA has been recognized as Consolidated Research Group by the Catalan government (2017-SGR-1016). This research is supported by the Spanish Ministry of Economy and Competitiveness (RTI2018-094757-B-I00, MCIU/AEI/FEDER, UE; and MDM-2017-0767) and by Obra Social "La Caixa", under projects 2018-LC-01 and 2019-URL-IR1rQ-011. G. Alonso thanks the University of Barcelona for his predoctoral APIF-2016 grant and P. Gamallo thanks Generalitat de Catalunya for his Serra Hünter Associate Professorship.

## REFERENCES

- [1] K.N. Marsh, J.A. Boxall, R. Lichtenthaler, Room Temperature Ionic Liquids and their Mixtures—a Review, *Fluid Phase Equilib.* 219 (2004) 93–98.
- [2] R.D. Rogers, K.R. Seddon, Ionic Liquids--Solvents of the Future?, *Science*. 302 (2003) 792–793.
- [3] T. Welton, Room-Temperature Ionic Liquids. Solvents for Synthesis and Catalysis, *Chem. Rev.* 99 (1999) 2071–2084.
- [4] S.N.V.K. Aki, B.R. Mellein, E.M. Saurer, J.F. Brennecke, High-Pressure Phase Behavior of Carbon Dioxide with Imidazolium-Based Ionic Liquids, *J. Phys. Chem. B.* 108 (2004) 20355–20365.
- [5] M.J. Muldoon, S.N.V.K. Aki, J.L. Anderson, J.K. Dixon, J.F. Brennecke, Improving Carbon Dioxide Solubility in Ionic Liquids, *J. Phys. Chem. B.* 111 (2007) 9001–9009.
- [6] J.E. Bara, C.J. Gabriel, S. Lessmann, T.K. Carlisle, A. Finotello, D.L. Gin, R.D. Noble, Enhanced CO<sub>2</sub> Separation Selectivity in Oligo(ethylene glycol) Functionalized Room-Temperature Ionic Liquids, *Ind. Eng. Chem. Res.* 46 (2007) 5380–5386.
- [7] O.M. Basha, M.J. Keller, D.R. Luebke, K.P. Resnik, B.I. Morsi, Development of a Conceptual Process for

Selective CO<sub>2</sub> Capture from Fuel Gas Streams Using [hmim][Tf<sub>2</sub>N] Ionic Liquid as a Physical Solvent, *Energ. Fuel.* 27 (2013) 3905–3917.

[8] M.B. Shiflett, A. Yokozeki, Solubility of CO<sub>2</sub> in Room Temperature Ionic Liquid [hmim][Tf<sub>2</sub>N], *J. Phys. Chem. B.* 111 (2007) 2070–2074.

[9] G. Alonso, D. Bahamon, F. Keshavarz, X. Giménez, P. Gamallo, R. Sayós, Density Functional Theory-Based Adsorption Isotherms for Pure and Flue Gas Mixtures on Mg-MOF-74. Application in CO<sub>2</sub> Capture Swing Adsorption Processes, *J. Phys. Chem. C.* 122 (2018) 3945–3957.

[10] W.G. Chapman, K.E. Gubbins, G. Jackson, M. Radosz, New Reference Equation of State for Associating Liquids, *Ind. Eng. Chem. Res.* 29 (1990) 1709–1721.

[11] S.H. Huang, M. Radosz, Equation of State for Small, Large, Polydisperse, and Associating Molecules, *Ind. Eng. Chem. Res.* 29 (1990) 2284–2294.

[12] F.J. Blas, L.F. Vega, Thermodynamic Behaviour of Homonuclear and Heteronuclear Lennard-Jones Chains with Association Sites from Simulation and Theory, *Mol. Phys.* 92 (1997) 135–150.

[13] L.M.C. Pereira, V. Martins, K.A. Kurnia, M.B. Oliveira, A.M.A. Dias, F. Llovel, L.F. Vega, P.J. Carvalho, J.A.P. Coutinho, High pressure solubility of CH<sub>4</sub>, N<sub>2</sub>O and N<sub>2</sub> in 1-butyl-3-methylimidazolium dicyanamide: Solubilities, selectivities and soft-SAFT modeling, *J. Supercrit. Fluids.* 110 (2016) 56–64.

[14] L.M.C. Pereira, M.B. Oliveira, F. Llovel, L.F. Vega, J.A.P. Coutinho, Assessing the N<sub>2</sub>O/CO<sub>2</sub> High Pressure Separation Using Ionic Liquids with the soft-SAFT EoS, *J. Supercrit. Fluids.* 92 (2014) 231–241.

[15] G. Zarca, I. Ortiz, A. Urtiaga, F. Llovel, Accurate Thermodynamic Modeling of Ionic Liquids/Metal Salt Mixtures: Application to Carbon Monoxide Reactive Absorption, *AIChE J.* 63 (2017) 3532–3543.

[16] M.B. Oliveira, F. Llovel, J.A.P. Coutinho, L.F. Vega, Modeling the [NTf<sub>2</sub>] Pyridinium Ionic Liquids Family and Their Mixtures with the Soft Statistical Associating Fluid Theory Equation of State, *J. Phys. Chem. B.* 116 (2012) 9089–9100.

[17] F. Llovel, M.B. Oliveira, J.A.P. Coutinho, L.F. Vega, Solubility of Greenhouse and Acid Gases on the [C<sub>4</sub>mim][MeSO<sub>4</sub>] Ionic Liquid for Gas Separation and CO<sub>2</sub> Conversion, *Catal. Today.* 255 (2015) 87–96.

[18] R.M. Ojeda, F. Llovel, Soft-SAFT Transferable Molecular Models for the Description of Gas Solubility in Eutectic Ammonium Salt-Based Solvents, *J. Chem. Eng. Data.* 63 (2018) 2599–2612.

[19] J.O. Lloret, L.F. Vega, F. Llovel, Accurate Description of Thermophysical Properties of Tetraalkylammonium Chloride Deep Eutectic Solvents with the soft-SAFT Equation of State, *Fluid Phase Equilibr.* 448 (2017) 81–93.

[20] E.A. Crespo, L.P. Silva, J.O. Lloret, P.J. Carvalho, L.F. Vega, F. Llovel, J.A.P. Coutinho, A methodology to parameterize SAFT-type equations of state for solid precursors of deep eutectic solvents: the example of cholinium chloride, *Phys. Chem. Chem. Phys.* 21 (2019) 15046–15061.

[21] A. Klamt, G. Schüürmann, COSMO: a New Approach to Dielectric Screening in Solvents with Explicit Expressions for the Screening Energy and its Gradient, *J. Chem. Soc. Perkin Trans. 2.* 0 (1993) 799–805.

[22] A. Klamt, Conductor-like Screening Model for Real Solvents: A New Approach to the Quantitative Calculation of Solvation Phenomena, *J. Phys. Chem.* 99 (1995) 2224–2235.

[23] C.B. Bavoh, B. Lal, O. Nashed, M.S. Khan, L.K. Keong, Mohd.A. Bustam, COSMO-RS: An Ionic Liquid Prescreening Tool for Gas Hydrate Mitigation, *Chin. J. Chem. Eng.* 24 (2016) 1619–1624.

- [24] Z. Lei, C. Dai, B. Chen, Gas Solubility in Ionic Liquids, *Chem. Rev.* 114 (2014) 1289–1326.
- [25] X. Zhang, Z. Liu, W. Wang, Screening of Ionic liquids to Capture CO<sub>2</sub> by COSMO-RS and Experiments, *AIChE J.* 54 (2008) 2717–2728.
- [26] F. Mozaffari, S.M.R. Mousavi, PVT properties of imidazolium-, phosphonium-, pyridinium- and pyrrolidinium-based ionic liquids using critical point constants, *Phys. Chem. Liq.* 55 (2017) 11–18.
- [27] F. Mozaffari, Modeling the volumetric properties of some imidazolium and phosphonium based ionic liquids from surface tension, *J. Mol. Liq.* 212 (2015) 461–466.
- [28] C.E. Ferreira, N.M.C. Talavera-Prieto, I.M.A. Fonseca, A.T.G. Portugal, A.G.M. Ferreira, Measurements of pVT, viscosity, and surface tension of trihexyltetradecylphosphonium tris(pentafluoroethyl)trifluorophosphate ionic liquid and modelling with equations of state, *J. Chem. Thermodyn.* 47 (2012) 183–196.
- [29] L.I.N. Tomé, R.L. Gardas, P.J. Carvalho, M.J. Pastoriza-Gallego, M.M. Piñeiro, J.A.P. Coutinho, Measurements and Correlation of High-Pressure Densities of Phosphonium Based Ionic Liquids, *J. Chem. Eng. Data.* 56 (2011) 2205–2217.
- [30] S.M. Hosseini, J. Moghadasi, M.M. Papari, F. Fadaei Nobandegani, Modeling the Volumetric Properties of Ionic Liquids Using Modified Perturbed Hard-Sphere Equation of State: Application to Pure and Binary Mixtures, *Ind. Eng. Chem. Res.* 51 (2012) 758–766.
- [31] T. Banerjee, A. Khanna, Infinite Dilution Activity Coefficients for Trihexyltetradecyl Phosphonium Ionic Liquids: Measurements and COSMO-RS Prediction, *J. Chem. Eng. Data.* 51 (2006) 2170–2177.
- [32] P.J. Carvalho, V.H. Álvarez, I.M. Marrucho, M. Aznar, J.A.P. Coutinho, High Carbon Dioxide Solubilities in Trihexyltetradecylphosphonium-Based Ionic Liquids, *J. Supercrit. Fluids.* 52 (2010) 258–265.
- [33] M.S. Manic, A.J. Queimada, E.A. Macedo, V. Najdanovic-Visak, High-pressure solubilities of carbon dioxide in ionic liquids based on bis(trifluoromethylsulfonyl)imide and chloride, *J. Supercrit. Fluids.* 65 (2012) 1–10.
- [34] M. Ramdin, T.Z. Olasagasti, T.J.H. Vlugt, T.W. de Loos, High pressure solubility of CO<sub>2</sub> in non-fluorinated phosphonium-based ionic liquids, *J. Supercrit. Fluids.* 82 (2013) 41–49.
- [35] D. Camper, P. Scovazzo, C. Koval, R. Noble, Gas Solubilities in Room-Temperature Ionic Liquids, *Ind. Eng. Chem. Res.* 43 (2004) 3049–3054.
- [36] P. Scovazzo, D. Camper, J. Kieft, J. Poshusta, C. Koval, R. Noble, Regular Solution Theory and CO<sub>2</sub> Gas Solubility in Room-Temperature Ionic Liquids, *Ind. Eng. Chem. Res.* 43 (2004) 6855–6860.
- [37] R.I. Canales, C. Held, M.J. Lubben, J.F. Brennecke, G. Sadowski, Predicting the Solubility of CO<sub>2</sub> in Toluene + Ionic Liquid Mixtures with PC-SAFT, *Ind. Eng. Chem. Res.* 56 (2017) 9885–9894.
- [38] M.S. Wertheim, Fluids with highly directional attractive forces. I. Statistical thermodynamics, *J. Stat. Phys.* 35 (1984) 19–34.
- [39] M.S. Wertheim, Fluids with highly directional attractive forces. II. Thermodynamic perturbation theory and integral equations, *J. Stat. Phys.* 35 (1984) 35–47.
- [40] M.S. Wertheim, Fluids with highly directional attractive forces. III. Multiple attraction sites, *J. Stat. Phys.* 42 (1986) 459–476.
- [41] M.S. Wertheim, Fluids with highly directional attractive forces. IV. Equilibrium polymerization, *J. Stat. Phys.* 42

(1986) 477–492.

- [42] F.J. Blas, L.F. Vega, Prediction of Binary and Ternary Diagrams Using the Statistical Associating Fluid Theory (SAFT) Equation of State, *Ind. Eng. Chem. Res.* 37 (1998) 660–674.
- [43] J. Gross, G. Sadowski, Perturbed-Chain SAFT: An Equation of State Based on a Perturbation Theory for Chain Molecules, *Ind. Eng. Chem. Res.* 40 (2001) 1244–1260.
- [44] A. Gil-Villegas, A. Galindo, P.J. Whitehead, S.J. Mills, G. Jackson, A.N. Burgess, Statistical associating fluid theory for chain molecules with attractive potentials of variable range, *J. Chem. Phys.* 106 (1997) 4168–4186.
- [45] A. Lymperiadis, C.S. Adjiman, A. Galindo, G. Jackson, A group contribution method for associating chain molecules based on the statistical associating fluid theory (SAFT- $\gamma$ ), *J. Chem. Phys.* 127 (2007) 234903:1–22.
- [46] F. Llovell, E. Valente, O. Vilaseca, L.F. Vega, Modeling Complex Associating Mixtures with [C<sub>n</sub>-mim][Tf<sub>2</sub>N] Ionic Liquids: Predictions from the Soft-SAFT Equation, *J. Phys. Chem. B.* 115 (2011) 4387–4398.
- [47] J.K. Johnson, J.A. Zollweg, K.E. Gubbins, The Lennard-Jones equation of state revisited, *Mol. Phys.* 78 (1993) 591–618.
- [48] K.E. Gubbins, C.H. Twu, Thermodynamics of polyatomic fluid mixtures—I theory, *Chem. Eng. Sci.* 33 (1978) 863–878.
- [49] P.K. Jog, S.G. Sauer, J. Blaesing, W.G. Chapman, Application of Dipolar Chain Theory to the Phase Behavior of Polar Fluids and Mixtures, *Ind. Eng. Chem. Res.* 40 (2001) 4641–4648.
- [50] F. Llovell, L.F. Vega, Prediction of Thermodynamic Derivative Properties of Pure Fluids through the Soft-SAFT Equation of State, *J. Phys. Chem. B.* 110 (2006) 11427–11437.
- [51] Y. Le Guennec, R. Privat, J.-N. Jaubert, Development of the translated-consistent tc-PR and tc-RK cubic equations of state for a safe and accurate prediction of volumetric, energetic and saturation properties of pure compounds in the sub- and super-critical domains, *Fluid Phase Equilibr.* 429 (2016) 301–312.
- [52] J.D. van der Waals, Thermodynamische Theorie der Kapillarität unter Voraussetzung Stetiger Dichteänderung, *Z. Für Phys. Chem.* 13 (1894) 657–725.
- [53] J.D. van der Waals, The Thermodynamic Theory of Capillarity under the Hypothesis of a Continuous Variation of Density, *J. Stat. Phys.* 20 (1979) 200–244.
- [54] J.W. Cahn, J.E. Hilliard, Free Energy of a Nonuniform System. I. Interfacial Free Energy, *J. Chem. Phys.* 28 (1958) 258–267.
- [55] C.C. Pye, T. Ziegler, E. van Lenthe, J.N. Louwen, An Implementation of the Conductor-Like Screening Model of Solvation within the Amsterdam Density Functional Package — Part II. COSMO for Real Solvents, *Can. J. Chem.* 87 (2009) 790–797.
- [56] ADF2017 COSMO-RS, SCM, Theoretical Chemistry, Vrije Universiteit, Amsterdam, The Netherlands, <http://www.scm.com>, n.d. <http://www.scm.com>.
- [57] T. Aissaoui, I.M. AlNashef, Y. Benguerba, Dehydration of natural gas using choline chloride based deep eutectic solvents: COSMO-RS prediction, *J. Nat. Gas Sci. Eng.* 30 (2016) 571–577.
- [58] T. Aissaoui, I.M. AlNashef, COSMO-RS Prediction for Choline Chloride/Urea Based Deep Eutectic Solvent: Chemical Structure and Application as Agent for Natural Gas Dehydration, 11 (2017) 9–12.

- [59] A.S.L. Gouveia, F.S. Oliveira, K.A. Kurnia, I.M. Marrucho, Deep Eutectic Solvents as Azeotrope Breakers: Liquid–Liquid Extraction and COSMO-RS Prediction, *ACS Sustain. Chem. Eng.* 4 (2016) 5640–5650.
- [60] K.Z. Sumon, A. Henni, Ionic liquids for CO<sub>2</sub> capture using COSMO-RS: Effect of Structure, Properties and Molecular Interactions on Solubility and Selectivity, *Fluid Phase Equilibr.* 310 (2011) 39–55.
- [61] R. Anantharaj, T. Banerjee, COSMO-RS-Based Screening of Ionic Liquids as Green Solvents in Denitrification Studies, *Ind. Eng. Chem. Res.* 49 (2010) 8705–8725.
- [62] J.P. Gutiérrez, G.W. Meindersma, A.B. de Haan, COSMO-RS-Based Ionic-Liquid Selection for Extractive Distillation Processes, *Ind. Eng. Chem. Res.* 51 (2012) 11518–11529.
- [63] A. Klamt, V. Jonas, T. Bürger, J.C.W. Lohrenz, Refinement and Parametrization of COSMO-RS, *J. Phys. Chem. A.* 102 (1998) 5074–5085.
- [64] B.P.M. Clapeyron, la puissance motrice de la chaleur, *J. L'École Polytech.* 14 (1834) 153–190.
- [65] N. Mac Dowell, F. Llovel, N. Sun, J.P. Hallett, A. George, P.A. Hunt, T. Welton, B.A. Simmons, L.F. Vega, New Experimental Density Data and Soft-SAFT Models of Alkylimidazolium ([C<sub>n</sub>C<sub>1</sub>im]<sup>+</sup>) Chloride (Cl<sup>-</sup>), Methylsulfate ([MeSO<sub>4</sub>]<sup>-</sup>), and Dimethylphosphate ([Me<sub>2</sub>PO<sub>4</sub>]<sup>-</sup>) Based Ionic Liquids, *J. Phys. Chem. B.* 118 (2014) 6206–6221.
- [66] A.M.A. Dias, H. Carrier, J.L. Daridon, J.C. Pàmies, L.F. Vega, J.A.P. Coutinho, I.M. Marrucho, Vapor–Liquid Equilibrium of Carbon Dioxide–Perfluoroalkane Mixtures: Experimental Data and SAFT Modeling, *Ind. Eng. Chem. Res.* 45 (2006) 2341–2350.
- [67] F. Llovel, R.M. Marcos, N. MacDowell, L.F. Vega, Modeling the Absorption of Weak Electrolytes and Acid Gases with Ionic Liquids Using the Soft-SAFT Approach, *J. Phys. Chem. B.* 116 (2012) 7709–7718.
- [68] J.S. Andreu, L.F. Vega, Capturing the Solubility Behavior of CO<sub>2</sub> in Ionic Liquids by a Simple Model, *J. Phys. Chem. C.* 111 (2007) 16028–16034.
- [69] J.S. Andreu, L.F. Vega, Modeling the Solubility Behavior of CO<sub>2</sub>, H<sub>2</sub>, and Xe in [C<sub>n</sub>-mim][Tf<sub>2</sub>N] Ionic Liquids, *J. Phys. Chem. B.* 112 (2008) 15398–15406.
- [70] J.M.S.S. Esperança, H.J.R. Guedes, M. Blesic, L.P.N. Rebelo, Densities and Derived Thermodynamic Properties of Ionic Liquids. 3. Phosphonium-Based Ionic Liquids over an Extended Pressure Range, *J. Chem. Eng. Data.* 51 (2006) 237–242.
- [71] E.A. Crespo, J.M.L. Costa, Z.B.M.A. Hanafiah, K.A. Kurnia, M.B. Oliveira, F. Llovel, L.F. Vega, P.J. Carvalho, J.A.P. Coutinho, New Measurements and Modeling of High Pressure Thermodynamic Properties of Glycols, *Fluid Phase Equilibr.* 436 (2017) 113–123.
- [72] P. Kilaru, G.A. Baker, P. Scovazzo, Density and Surface Tension Measurements of Imidazolium-, Quaternary Phosphonium-, and Ammonium-Based Room-Temperature Ionic Liquids: Data and Correlations, *J. Chem. Eng. Data.* 52 (2007) 2306–2314.
- [73] S. Zeng, X. Zhang, L. Bai, X. Zhang, H. Wang, J. Wang, D. Bao, M. Li, X. Liu, S. Zhang, Ionic-Liquid-Based CO<sub>2</sub> Capture Systems: Structure, Interaction and Process, *Chem. Rev.* 117 (2017) 9625–9673.
- [74] L. Ferguson, P. Scovazzo, Solubility, Diffusivity, and Permeability of Gases in Phosphonium-Based Room Temperature Ionic Liquids: Data and Correlations, *Ind. Eng. Chem. Res.* 46 (2007) 1369–1374.
- [75] J. Jacquemin, P. Husson, V. Majer, M.F.C. Gomes, Low-Pressure Solubilities and Thermodynamics of Solvation of Eight Gases in 1-Butyl-3-Methylimidazolium Hexafluorophosphate, *Fluid Phase Equilibr.* 240 (2006) 87–95.

- [76] J. Jacquemin, M.F. Costa Gomes, P. Husson, V. Majer, Solubility of Carbon Dioxide, Ethane, Methane, Oxygen, Nitrogen, Hydrogen, Argon, and Carbon Monoxide in 1-Butyl-3-Methylimidazolium Tetrafluoroborate Between Temperatures 283K and 343K and at Pressures Close to Atmospheric, *J. Chem. Thermodyn.* 38 (2006) 490–502.
- [77] D. Camper, C. Becker, C. Koval, R. Noble, Low Pressure Hydrocarbon Solubility in Room Temperature Ionic Liquids Containing Imidazolium Rings Interpreted Using Regular Solution Theory, *Ind. Eng. Chem. Res.* 44 (2005) 1928–1933.
- [78] M.F. Friedrich, S. Kokolakis, M. Lucas, P. Claus, Measuring Diffusion and Solubility of Slightly Soluble Gases in  $[C_n\text{MIM}][\text{NTf}_2]$  Ionic Liquids, *J. Chem. Eng. Data.* 61 (2016) 1616–1624.
- [79] D. Camper, C. Becker, C. Koval, R. Noble, Diffusion and Solubility Measurements in Room Temperature Ionic Liquids, *Ind. Eng. Chem. Res.* 45 (2006) 445–450.
- [80] A. Finotello, J.E. Bara, D. Camper, R.D. Noble, Room-Temperature Ionic Liquids: Temperature Dependence of Gas Solubility Selectivity, *Ind. Eng. Chem. Res.* 47 (2008) 3453–3459.